Hindawi Publishing Corporation
Journal of Nanomaterials
Volume 2013, Article ID 425071, 10 pages
http://dx.doi.org/10.1155/2013/425071

Research Article

Effects of Ar or O_2 Gas Bubbling for Shape, Size, and Composition Changes in Silver-Gold Alloy Nanoparticles Prepared from Galvanic Replacement Reaction

Md. Jahangir Alam[1] and Masaharu Tsuji[2]

[1] *Department of Agronomy and Agricultural Extension, Rajshahi University, Rajshahi 6205, Bangladesh*
[2] *Institute for Materials Chemistry and Engineering, Kyushu University, Kasuga 816-8580, Japan*

Correspondence should be addressed to Md. Jahangir Alam; jahangir9392004@yahoo.com

Received 13 June 2013; Accepted 15 August 2013

Academic Editor: Shuangxi Xing

The galvanic replacement reaction between silver nanostructures and $AuCl_4^-$ solution has recently been demonstrated as a versatile method for generating metal nanostructures with hollow interiors. Here we describe the results of a systematic study detailing the morphological, structural, compositional, and spectral changes involved in such a heterogeneous reaction on the nanoscale. Effects of Ar or O_2 gas bubbling for the formation of Ag-Au alloy nanoparticles by the galvanic replacement between spherical Ag nanoparticles and $AuCl_4^-$ especially were studied in ethylene glycol (EG) at 150°C. The shape, size, and composition changes occur rapidly under O_2 bubbling in comparison with those under Ar bubbling. The major product after 60 min heating under Ar gas bubbling was perforated Ag-Au alloy particles formed by the replacement reaction and the minor product was ribbon-type particles produced from splitting off some perforated particles. On the other hand, the major product after 60 min heating under O_2 gas bubbling was ribbon-type particles. In addition, small spherical Ag particles are produced. They are formed through rereduction of Ag^+ ions released from the replacement reaction and oxidative etching of Ag nanoparticles by O_2/Cl^- in EG.

1. Introduction

The properties of alloy nanoparticles are significantly different from those of individual monometallic nanoparticles [1, 2]. This provides yet another dimension in tailoring the properties of nanomaterials besides the usual size and shape manipulation. For example, Ag-Au alloy nanoparticles are more catalytically active than monometallic Ag or Au nanoparticles in the oxidation of CO at low temperatures [3, 4]. In addition, while monometallic spherical Ag and Au nanoparticles have relatively unchanging optical properties due to surface plasmon resonance (SPR), the SPR properties of Ag-Au alloy nanoparticles are continuously tunable because of the possibility of composition changes [5]. Although Ag-Au alloy nanoparticles can be prepared by a number of methods, the most common one is the coreduction of the corresponding metal precursor salts in the presence of a stabilizing agent [6–11]. Water in oil microemulsions has also been used by Chen to produce Ag-Au alloy nanoparticles [12]. In the digestive ripening method of Smetana and coworkers [13], Ag-Au alloy nanoparticles were formed by refluxing Ag and Au nanoparticles in 4-tertbutyltoluene in the presence of an alkanethiol. Other methods of preparation of a more physical nature include laser ablation [14–16] and evaporation condensation [17]. Despite a myriad of methods of preparation, the large-scale synthesis of alloy nanoparticles with good control of size and composition remains a challenge. First, size tuning by changing the synthesis conditions is more complex for the alloy nanoparticles than for the monometallic nanoparticles. This is because the synthesis conditions affect the reduction potentials and the effectiveness of the stabilizing agent in different ways. Second, most current methods of preparation are unable to decouple shape, size, and composition control, which increases the

difficulty in producing alloy nanoparticles with the same composition but different sizes, or the same size with different compositions. In addition, Ag^+ ions have the propensity of forming insoluble halide precipitates whenever the synthesis involves the use of a halogen containing metal precursor salt (e.g., $HAuCl_4$). The precipitation of AgCl contaminates the alloy nanoparticles formed and further complicates the control of alloy composition.

Herein we report a simple method to prepare Ag-Au alloy nanoparticles by the replacement reaction between Ag nanoparticles and $AuCl_4^-$ at a high temperature of 150°C under Ar or O_2 gas bubbling. While this method bears certain similarities with the works of Xia and other researchers [18–21], the synthesis conditions were altered to deliberately suppress the formation of hollow structures. This method takes advantage of the rapid interdiffusion of Au and Ag atoms in the reduced dimension of nanoparticles, relatively lower temperature of operation, and the large number of interfacial vacancy defects created by the replacement reaction. The major advantages of this method are that the shape, size, and composition of the alloy nanoparticles are independently tunable and that the particles can be produced in high concentrations. Here, we report a polyol synthesis of monodisperse Ag-Au alloy nanoparticles through the galvanic replacement reaction between Ag atoms and $AuCl_4^-$ under gas bubbling. We first prepared spherical/decahedron Ag nanoparticles by thermal reduction of $AgNO_3$ in ethylene glycol (EG) under Ar gas bubbling in the presence of polyvinylpyrrolidone (PVP) for 50 min heating. These Ag nanoparticles were then used as seeds (sacrificial template) on which Au was deposited by reduction of $HAuCl_4$ in EG under Ar or O_2 gas bubbling at 150°C. Spherical Ag seeds for the galvanic replacement reaction with $HAuCl_4$ in EG at 150°C lead to various shapes of Ag-Au alloy nanoparticles. In the synthesis, EG and PVP are used as reducing agent and stabilizing surfactant, respectively.

Xia's and Mirkin's groups developed a one-step approach based on galvanic replacement reaction that was capable of generating hollow nanostructures consisting of various metals such as Au, Pd, and Pt [22–25]. In a typical procedure, Ag nanoparticles were used as sacrificial templates to react with $HAuCl_4$ solution in EG, resulting in the formation of Ag-Au nanoshells with hollow interiors, as well as heterogeneous and highly crystalline walls. However, a detailed account of the morphological, structural, compositional, and spectral changes involved in the replacemen reaction needs to be provided.

Our present results clearly demonstrated that the template engaged replacement reaction proceeded through two distinctive steps: (i) the formation of seamless hollow structures (with the walls made of Ag-Au alloys) via a combination of galvanic replacement between Ag and $AuCl_4^-$ and alloying (between Au and Ag) under Ar gas bubbling and (ii) the formation of hollow structures with slightly broken shapes and small ribbon-type nanoparticles under O_2 gas bubbling due to oxidative etching. The formation mechanisms of Ag-Au alloys under gas bubbling are discussed in terms of galvanic replacement reaction and oxidative etching.

2. Experimental Section

2.1. Materials and Experimental Procedures. For use in this study, $HAuCl_4{\cdot}4H_2O$ (>99.0%), $AgNO_3$ (>99.8%), and EG (>99.5%) were purchased from Kishida Chemical Co., Ltd. The PVP powder (average molecular weight M_W: 40 k) was purchased from Wako Pure Chemical Industries Ltd. All these reagents were used without further purification. Oxygen (>99.9%) and Argon (>99.9995%) gases were obtained from Taiyo Nippon Sanso Corp.

Preparation of Ag seeds: 15 mL of EG solution was preheated at 150°C and maintained at this temperature for 60 min by Ar gas bubbling. Then a mixture of $AgNO_3$ and PVP (M_W = 40 k) as a polymer surfactant in 5 mL of EG was added and further heated at 150°C for 50 min under Ar gas bubbling. The concentrations of $AgNO_3$ and PVP in 20 mL EG were 24 mM and 250 mM (in terms of monomeric units), respectively. The products were collected by centrifugal separation at 12,000 rpm three times for 30 min to remove all byproducts produced in the supernatant. These Ag nanoparticles were used as seeds for the galvanic replacement reaction shown in Section 2.2.

2.2. Shape and Component Changes in Products by the Addition of Ag Particles to $HAuCl_4{\cdot}4H_2O$/PVP/EG Solution under Ar or O_2 Gas Bubbling. About 5 mL of EG solution containing 9.6 mM $HAuCl_4{\cdot}4H_2O$ was injected to 15 mL of EG solution containing all Ag seeds and 250 mM PVP. It was heated from room temperature to 150°C for 6 min; it was kept at that temperature for 60 min with sampling at 10, 30, and 60 min under Ar or O_2 gas bubbling. The total flow rate of bubbling gas was kept at 150 sccm using mass flow controllers. The final concentrations of $HAuCl_4{\cdot}4H_2O$, Ag atoms in seeds, and PVP in 20 mL EG were 2.4, 24, and 250 mM, respectively.

2.3. Analyses of Shape, Component, and Optical Properties of Products. For TEM (200 kV, JEM-2000XS; JEOL) observations, Ag and Ag-Au bimetallic particles were obtained from C_2H_5OH solution by centrifuging the colloidal solution at 15,000 rpm for 30 min three times. The TEM energy dispersed X-ray spectroscopy (EDS) data were also measured (200 kV, 2100F; JEOL). XRD patterns of powder samples were measured (SmartLab with Cu Ka radiation operating at 45 kV and 200 mA; Rigaku). Extinction spectra of the product solutions were measured in the UV-Vis region using a spectrometer (UV-3600; Shimadzu Corp.). The samples were diluted with EG before observation.

3. Result and Discussion

3.1. Galvanic Replacement Reaction between Ag and $AuCl_4^-$. Galvanic replacement reaction has been demonstrated as a general and effective means for preparing metallic nanostructures (e.g., thin films) by consuming the more reactive component [26, 27]. We have focused on spherical/decahedron Ag particles because this class of nanostructures provides a model system with monodispersed size and well-defined facets. Since the standard reduction potential of $AuCl_4^-$/Au

pair (0.99 V versus standard hydrogen electrode, SHE) is higher than that of the Ag^+/Ag pair (0.80 V versus SHE), silver would be oxidized into Ag^+, when silver nanostructures and $HAuCl_4$ are mixed in organic polyol medium as

$$3Ag + AuCl_4^- \longrightarrow Au + 3Ag^+ + 4Cl^-. \quad (1)$$

Both TEM and TEM-EDS images were used to follow the shape, size, and composition changes involved in various stages of the replacement reaction between spherical/decahedron Ag particles (templates) and $HAuCl_4$ solution.

3.2. Shape and Component Changes in Products by the Addition of Ag Particles to $HAuCl_4$/PVP/EG Solution under Ar Bubbling. Figure 1 depicts TEM images of Ag nanoparticles (all started with the same amount) before and after they had reacted with 2.4 mM $HAuCl_4$ at 150°C for 10–60 min under Ar gas bubbling. Most of Ag seed particles are twin particles (decahedron) in which twin lines appeared under oil-bath heating of $AgNO_3$/PVP (40 K)/EG solution under Ar gas bubbling at 150°C for 50 min (Figure 1(a), see also Figure S1 in Supplementary Material available at http://dx.doi.org/10.1155/2013/425071). The average diameter of Ag seeds which consist of a mixture of spherical/decahedral particles was 38 ± 15 nm. We used oil-bath heating for the synthesis of Ag-Au alloy particles using a mixture of theses Ag seeds as a sacrificial template and $HAuCl_4$/PVP in EG solution under Ar gas bubbling at 150°C.

After the Ag structures had reacted with $HAuCl_4$ solution in the presence of PVP under Ar gas bubbling for 10 min at 150°C, a pin hole is formed at a specific site of the surface (Figure 1(b)), indicating that the replacement reaction was initiated locally rather than over the entire surface. The holes can be clearly observed as on the surfaces of spherical particles. This observation suggested that only one hole is formed on each particle because each polycrystalline particle has planer defect on its surfaces, from which the pin hole would be originated via replacement reaction. The newly formed surfaces containing holes should represent the most active sites for further replacement reaction. The dimensions of each particle exhibited no apparent change in the initial stage of this reaction, indicating that the gold atoms were deposited on the surface of each particle as a very thin (most likely, incomplete) shell.

Although reduction of $HAuCl_4$ by EG at 150°C leading to Au particles competes with the galvanic replacement reaction under the present experimental condition, dominant shapes of product particles are hollow particles and little pure Au particles are formed in any stage. This shows that the galvanic replacement reaction occurs preferentially to the thermal reduction of $HAuCl_4$ under the present conditions. In the typical synthesis of Ag-Au alloy nanoparticles, Au^{3+} cations are reduced by the metallic Ag nanoparticles and the Au atoms are deposited onto the Ag surface followed by a simultaneous mutual diffusion process between Au and Ag. Since three Ag atoms need to be sacrificed to reduce one Au^{3+} cation, the diffusion induces a large number of vacancies and voids in Ag nanoparticles, facilitating alloy formation [28]. In continuous heating process, we observed that the shape and size of products are changed gradually with increasing the heating time up to 60 min. After 30 min heating (Figure 1(c)), there is a small shape change in product particles. As a result, the replacement reaction could be continued to generate larger holes as compared to 10 min heating products. After 60 min heating (Figure 1(d)), some small ribbon-type particles are also prepared from splitting off some perforated particles due to more replacement reaction and creating much more pin hole inside particles. Larger porous particles turn to small ribbon-type particles for further diffusion process, whereas the number density of perforated particles decreases in Figure 1(d).

To obtain more information related to distributions of Au and Ag components in the product particles at different heating times, TEM-EDS measurements and line analysis were conducted for 10 min heating (Figures 2(a1)–2(e1)). These data clarify that the particles along diagonal lines are composed of Ag-rich Ag-Au alloys. The atomic ratio of Au : Ag for all particles shown in Figures 2(a1)–2(e1) was 27% : 73%, whereas that of a porous particle located in the center of Figures 2(a1)–2(d1) was 30% : 70%. This implies that more Ag particles were replaced by Au component in porous particles. After 30 min heating, the atomic ratio of Au : Ag for all particles shown in Figures 2(a2)–2(e2) was 40% : 60%, indicating a significant increase in the fraction of Au component due to more replacement reaction between Ag atoms and $AuCl_4^-$. After 60 min heating, the atomic ratio of Au : Ag for all particles in Figures 2(a3)–2(e3) was 42% : 58%, which is nearly the same as that at 30 min heating. This implies that most of replacement reaction is completed before 30 min under the present conditions under Ar gas bubbling. It is noteworthy that small Ag particles are formed during heating as shown in Supplementary Figure S2 with red circles. After galvanic replacement reaction, some Ag atoms are dissolved as Ag^+ ions and they are rereduced to small Ag particles by EG at 150°C.

To obtain information related to product particles, XRD patterns were measured for all particles, obtained after 60 min heating (Supplemntary Figure S3). Because of the same fcc crystal structure and similar lattice constants among Au, Ag, and AuAg metals (lattice mismatch <0.2%), XRD patterns of Au (PDF 00-071-4073), Ag (PDF 00-004-0783), and AuAg alloy (PDF 01-071-9134) show similar diffraction peaks, which are overlapped mutually. Prominent diffraction peaks in Supplemntary Figure S3 were indexed to the {111}, {200}, {220}, {311}, and {222} planes of a mixture of Ag-Au alloy and Ag particles with fcc structure. In addition, a weak peak corresponding to the {200} plane of AgCl particles (PDF 01–085-1355) was observed. The peak intensity of the {111} facet of Ag-Au alloy and Ag particles is the strongest, suggesting that the favorable facet of AgAu alloy and Ag particles is {111}. Sharp peaks observed for Ag-Au alloy and Ag particles without amorphous components suggest that these particles are composed of polycrystals. Since the peak intensity of AgCl is weak, the contribution of AgCl in the products is expected to be small. In our reaction system, a significant amount of AgCl having a very small solubility product at room temperature in EG may be formed

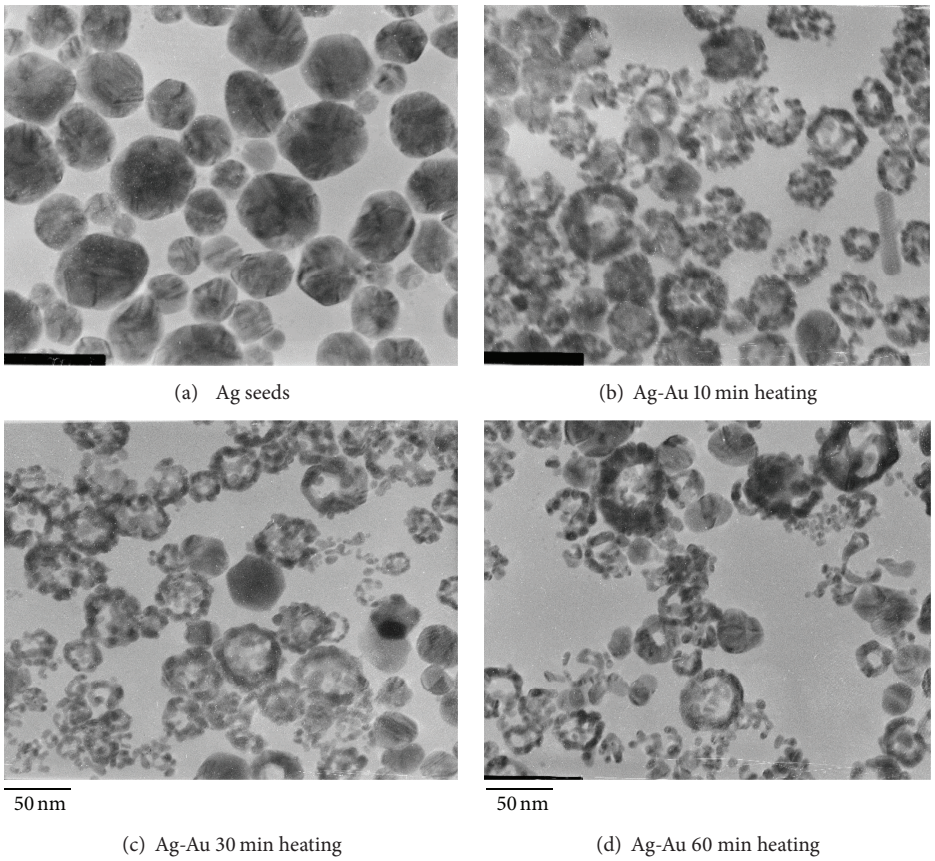

(a) Ag seeds (b) Ag-Au 10 min heating

(c) Ag-Au 30 min heating (d) Ag-Au 60 min heating

Figure 1: Typical TEM images of (a) polygonal Ag seeds and ((b)–(d)) Ag-Au bimetallic products after heating Ag seeds/$HAuCl_4$/PVP/EG solution for 10–60 min under Ar gas bubbling. Scale bars of TEM images (a) and (b) are the same as those of (c) and (d), respectively.

because Ag^+ ions are released from Ag by the replacement reaction, whereas Cl^- ions are formed by the decomposition of $HAuCl_4$. However, we found that the atomic content of Cl in Ag-Au-Cl products was only 1.4% on the basis of EDS and XRD data. The low AgCl content in product is attributed to dissolution of AgCl to Ag^+ to Cl^- during heating at a relatively high temperature of 150°C and rereduction of Ag^+ to Ag^0.

3.3. Shape and Component Changes in Products by the Addition of Ag Particles to $HAuCl_4$/PVP/EG Solution under O_2 Bubbling. Figure 3 portrays typical TEM images of Ag nanoparticles (all started with the same amount) before and after they had reacted with 2.4 mM $HAuCl_4$ in EG solution at 150°C under O_2 gas bubbling. Figure 3(a) depicts a typical TEM image of Ag seeds, where Ag particles with an average size of 32 ± 12 nm are observed. Figure 3(b) depicts a typical TEM image of products after heating at 150°C for 10 min under O_2 gas bubbling. There is a dramatically shape change occurring in this stage. Spherical Ag seeds turn to ring-type particles with a pin hole at upper surface area and a small amount of ribbon-type particles due to fast oxidative etching of Ag sacrificial template with the assistance of replacement reaction between Ag atoms and $AuCl_4^-$ ions. It should be noted that Ag particles are oxidized not only by the replacement reaction by $AuCl_4^-$ ions but also by oxidative etching by Cl^-/O_2 [29, 30] under O_2 gas bubbling and they are released as Ag^+ ions in solution at 150°C. After 30 min heating, the number density of the ribbon-type particles increased in comparison with that of the pinhole particles as shown in Figure 3(c). After 60 min heating, the residual perforated particles are further split off into small (collapsed into small fragments) ribbon-type particles, as shown in Figure 3(d).

For better understanding of Au and Ag atomic distributions in product particles under O_2 gas bubbling, EDS measurements were conducted and the results obtained for 10, 30, and 60 min heating are shown in Figures 4(a1)–4(e3), respectively. After 10 min heating, perforated ring-like particles and some small fragments of Ag-Au alloy are produced. Line analysis data shown in Figure 4(e1) along a blue line given in Figure 4(d1) suggest that product particles are composed of Ag-rich Ag-Au alloys. The Au : Ag atomic ratio for the all particles in Figures 4(a1)–4(d1) was 34% : 66%, indicating that Au content in product is higher than that under Ar gas bubbling at 10 min (27%). After 30 min heating, the Au : Ag atomic ratio was 44% : 56%. The Au content in Ag-Au alloy particles increases significantly with increasing the heating time. After 60 min heating, the volume of hole increases and porous particles are broken into small ribbon-type particles, as shown in Figures 4(a3)–4(d3). The Au : Ag atomic ratio was 52% : 48%. On the basis of the above

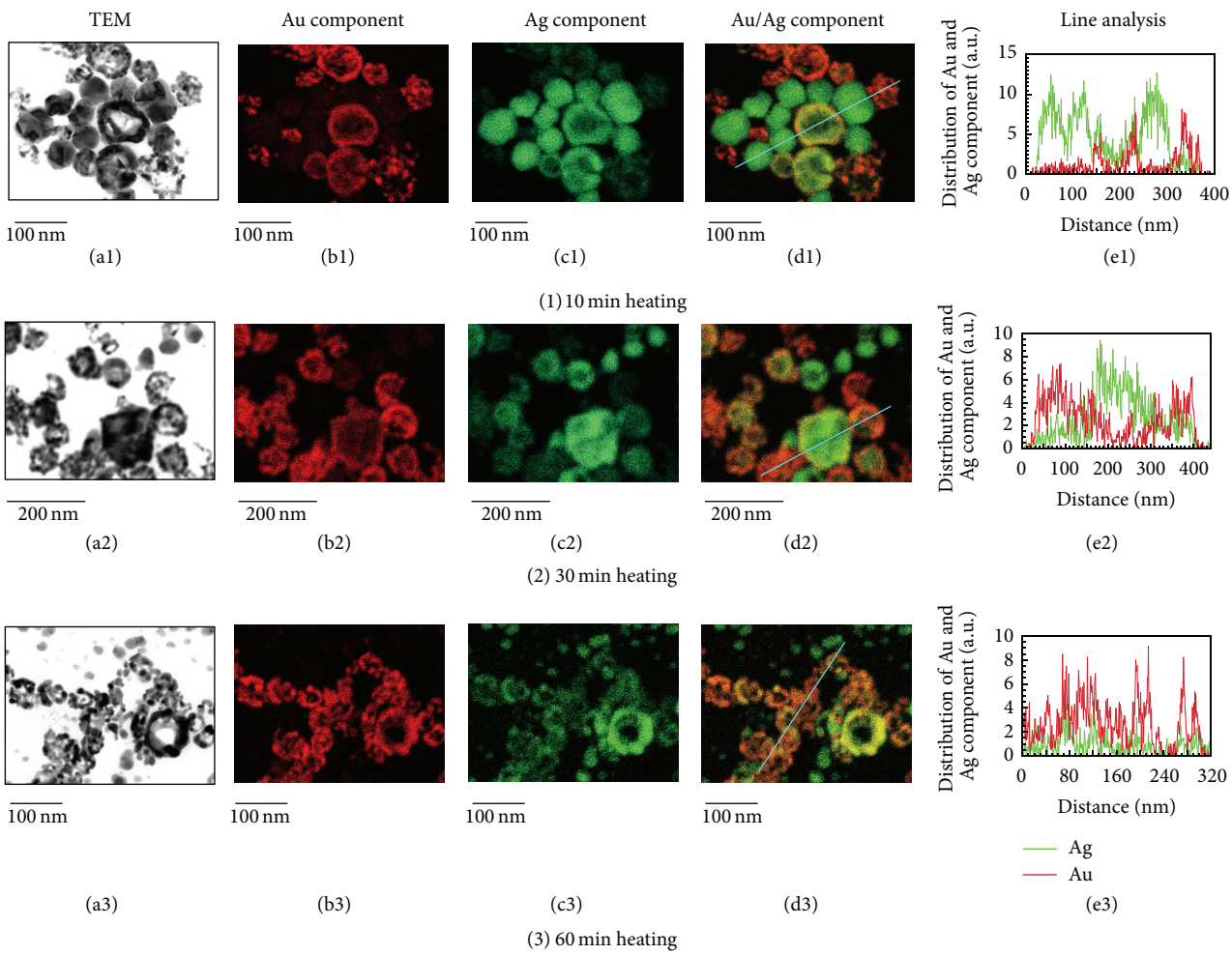

Figure 2: Typical TEM and TEM-EDS images of Ag-Au bimetallic products obtained after heating Ag seeds/$HAuCl_4$/PVP/EG solution for 10–60 min under Ar gas bubbling. Line analysis data along blue lines in (d1), (d2), and (d3) are given in (e1), (e2), and (e3), respectively.

findings, the Au content in Ag-Au alloy particles increases from 34% to 52% with increasing the reaction time from 10 min to 60 min. It should be noted that some small Ag particles (<5 nm) are created, as shown in Supplemntary Figure S4 with red circles. It is reasonable to assume that these small Ag nanoparticles arise from replacement reaction and oxidative etching of the original templates followed by rereduction of Ag^+ under O_2 gas bubbling. Oxidative etching of Ag particles occurs by O_2/Cl^- [29, 30], where Cl^- ions are formed by decomposition of $HAuCl_4$.

On the basis of TEM and TEM-EDS data given above, different shape, size, and composition of Ag-Au alloy particles are formed under Ar or O_2 bubbling at 150°C. Ag sacrificial templates are gradually changed to a mixture of ring-type perforated Ag-Au alloy and small ribbon particles under Ar gas bubbling during oil-bath heating for 60 min. On the other hand, Ag particles are changed to ring-type perforated particles in a short time and they are finally converted to small fragment species due to fast oxidative etching as well as galvanic replacement reaction between Ag atoms and $AuCl_4^-$ ions under O_2 gas bubbling. The XRD pattern of products under O_2 gas bubbling was similar to that under Ar gas, indicating that a similar mixture of Ag-Au alloy and Ag polycrystals was formed under O_2 gas bubbling.

3.4. Spectral Changes after Heating $HAuCl_4$/PVP/EG Solution in the Presence of Ag Seeds under Ar Gas Bubbling. We could also conveniently monitor the galvanic replacement reaction between spherical Ag particles and $HAuCl_4$ solution by spectroscopic means because nanostructures made of Au and Ag often exhibit distinctive SPR bands in the UV-Vis region. It is known that peak positions of Au and Ag SPR bands strongly depend on their shape and structure (e.g., solid versus hollow) [31–33]. Figures 5(a) and Supplemntary Figure S5a (expanded scale of Figure 5(a)) show extinction spectra recorded from EG dispersions of Ag nanoparticles after they are heated with $HAuCl_4$ solution at 150°C under Ar gas bubbling. For comparison, UV-Vis spectra of original Ag particles in EG are also shown. The SPR band of spherical Ag particles with a peak at ≈440 nm is observed in the 300–700 nm region. The spectral changes from Ag nanoparticles

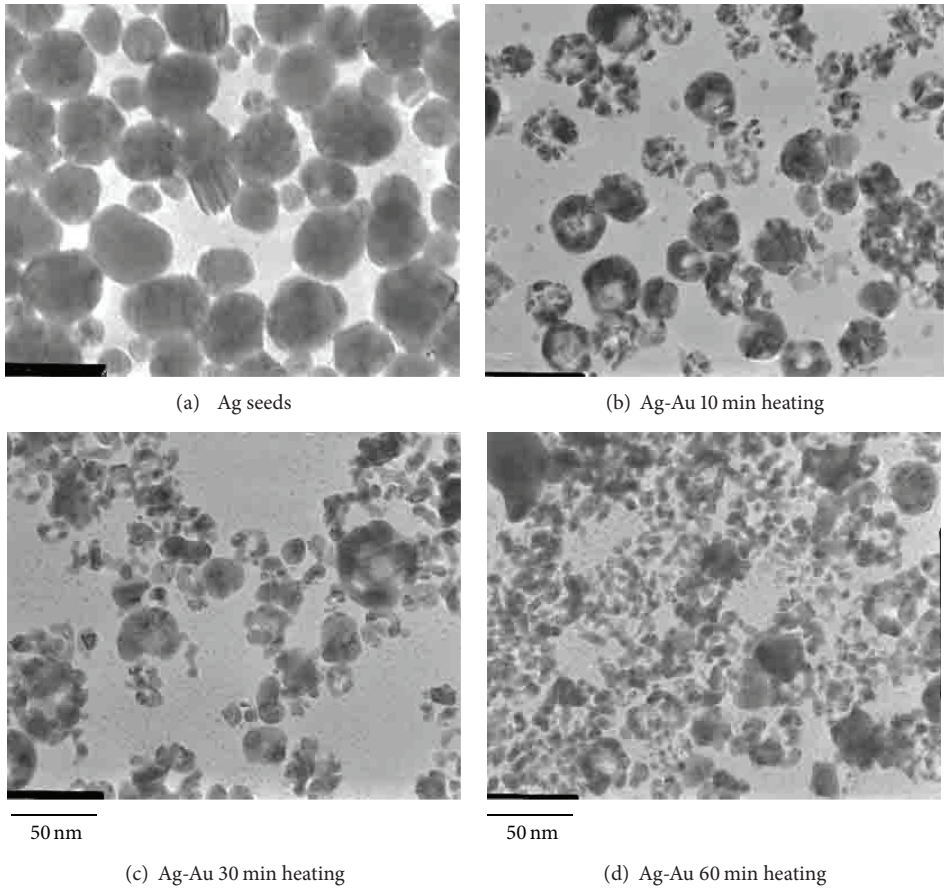

(a) Ag seeds (b) Ag-Au 10 min heating

(c) Ag-Au 30 min heating (d) Ag-Au 60 min heating

Figure 3: Typical TEM images of (a) polygonal Ag seeds and ((b)–(d)) Ag-Au bimetallic products after heating Ag seeds/$HAuCl_4$/PVP/EG solution for 10–60 min under O_2 gas bubbling. Scale bars of TEM images (a) and (b) are the same as those of (c) and (d), respectively.

to Ag-Au alloy particles are consistent with the formation of hollow ring-like nanoparticles with their walls composed of homogeneous Ag-Au alloys. After 10 min heating, the hollow Ag-Au alloy and ribbon-type particles exhibited a broad SPR band in the 300–800 nm region with a peak at ≈450 nm. This spectral change can be attributed to the deposition of thin Au layers on the surfaces of Ag templates, which is further transformed into thin shells of Ag-Au alloy particles. The peak at ≈450 nm for Ag particles decreases in intensity greatly after 10 min heating due to the formation of Ag-Au alloy particles. After 30–60 min heating, the intensity of peaks slightly increases and becomes broad indicating that Au^{3+} ions are reduced by Ag and constitute Ag-Au alloy around the pinhole with a porous shell. These results also indicate that the thickness of Ag-Au alloy decreases around holes in perforated Ag-Au alloy particles, with increasing the volume of holes. It is concluded that the small shift in peak position might be caused by the increase in void size and the reduction in wall thickness for the Ag-Au alloy. The reduction in wall thickness, which played an important role in determining the SPR features, might also be involved in the dealloying process. The broadening of the SPR bands arises from large particle sizes, their wider size distributions, and change in dielectric constant of Ag by the presence of Au.

3.5. Spectral Changes after Heating $HAuCl_4$/PVP/EG Solution in the Presence of Ag Seeds under O_2 Gas Bubbling. UV-Vis spectra were measured to characterize optical properties and to examine time evolution of Ag-Au alloy particles. Results obtained are shown in Figure 5(b) and Supplementary Figure S5b (expanded scale of Figure 5(b)). For comparison UV-Vis spectra of spherical Ag particles in EG are also shown. After injection of $HAuCl_4$ and heating for 10 min, the SPR band becomes weak and broad with a peak at ≈510 nm. This peak broadening is probably related to a wider range of void sizes in the resultant hollow nanostructures or Au rich discrete Ag-Au alloy particles. The intensity change of the SPR band in Figure 5(b) is opposite to that in Figure 5(a). Although the intensity of peaks slightly increased with an increase in heating time in Figure 5(a), it decreased with an increase in heating time in Figure 5(b). These spectral differences in peak positions and intensity changes are probably related to the higher Au content in the product Ag-Au alloys and higher amount of small ribbon-type particles under O_2 gas bubbling.

3.6. Mechanisms of Shape and Composition Changes in Ag-Au Bimetallic Systems under Ar or O_2 Gas Bubbling. It is an interesting observation that homogeneous Ag-Au alloy

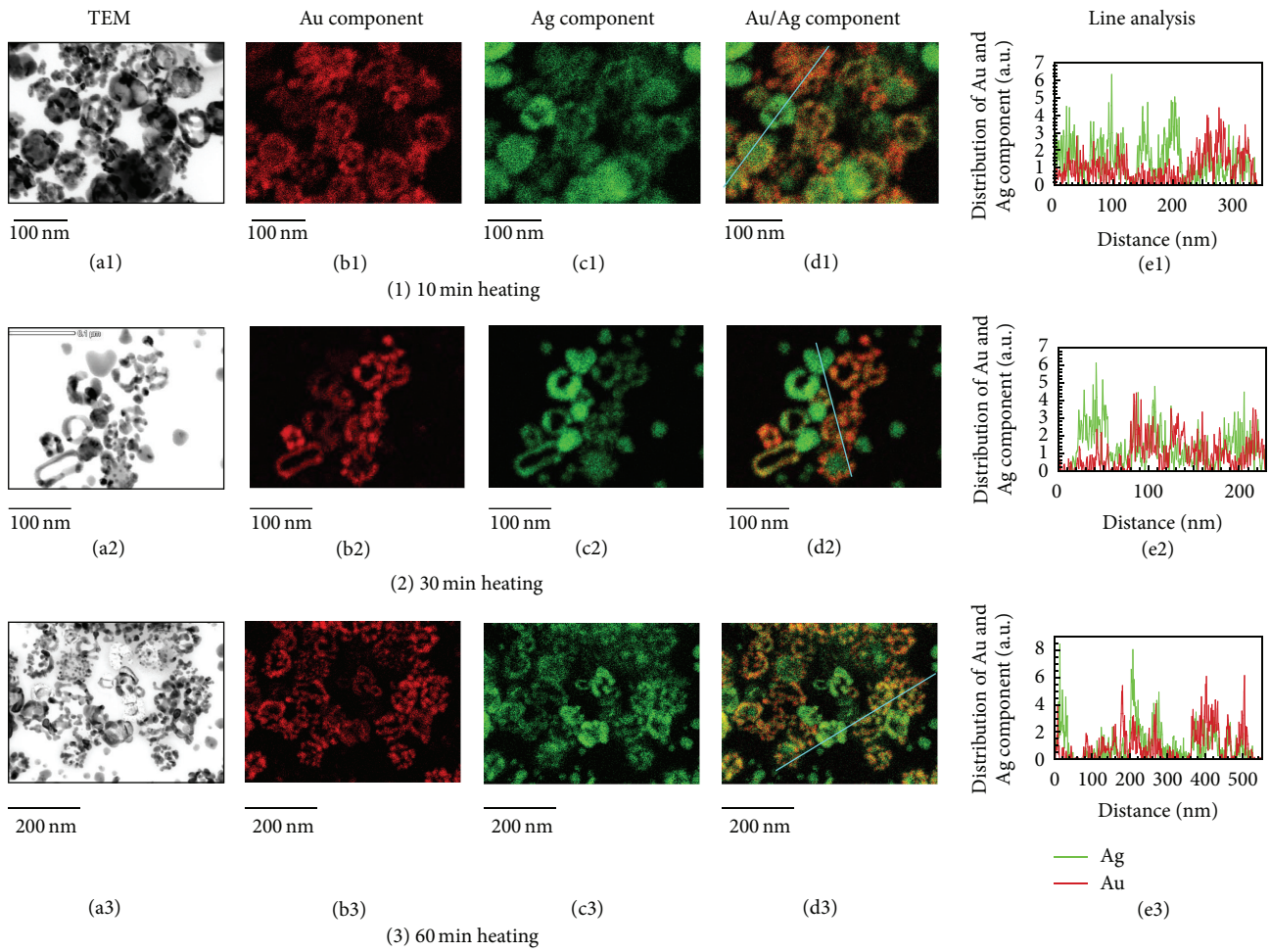

FIGURE 4: Typical TEM and TEM-EDS images of Ag-Au bimetallic products obtained after heating Ag seeds/$HAuCl_4$/PVP/EG solution under O_2 gas bubbling. Line analysis data along blue lines in (d1), (d2), and (d3) are given in (e1), (e2), and (e3), respectively.

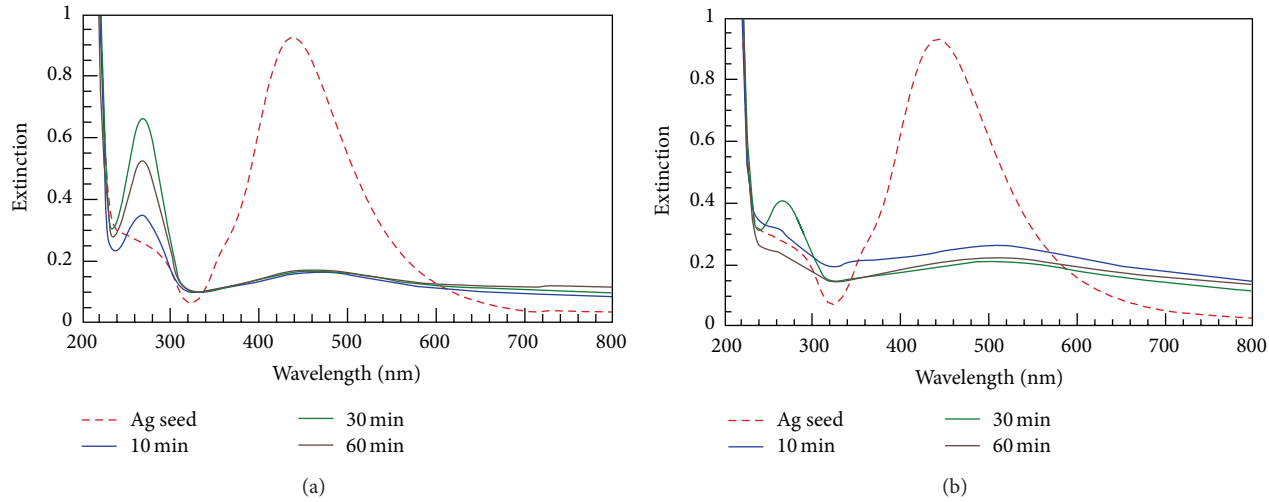

FIGURE 5: Spectral changes of Ag and Ag-Au bimetallic products obtained before and after heating Ag seeds/$HAuCl_4$/PVP/EG solution (a) under Ar gas bubbling (b) O_2 gas bubbling.

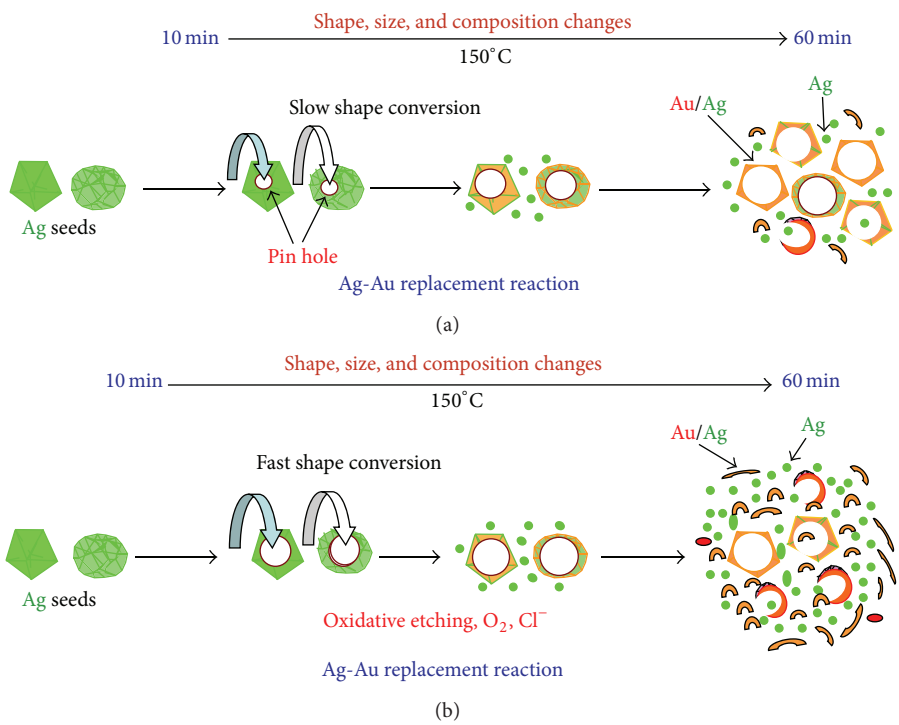

Figure 6: Schematic process for shape, size, and composition changes in Ag-Au bimetallic products obtained after heating Ag seeds/$HAuCl_4$/PVP/EG solution (a) under Ar gas bubbling and (b) under O_2 gas bubbling.

nanoparticles were formed as a result of the replacement reaction. This indicates that the alloying between Ag and Au was concurrent with the replacement reaction. It is known that a solid solution of Ag and Au is thermodynamically more stable than pure Au or Ag [34]. Alloy formation requires the interdiffusion of Au and Ag atoms, which is generally slow for bulk gold and silver. However, the rate of diffusion in metallic atoms can increase rapidly with the decrease in particle dimension and the presence of vacancy defects [35–42].

Figure 6(a) shows schematic process for shape, size, and composition changes from Ag nanoparticles to Ag-Au alloy particles under Ar gas bubbling after heating at 150°C for 10–60 min. As Ag seeds, decahedron and spherical Ag particles with average size of 38 ± 15 nm are used. By the addition of $HAuCl_4$ solution to the Ag seed solution in the presence of PVP under Ar gas bubbling, a pin hole is formed at a specific site of the surface especially at the planer defect of twin or polycrystalline particles. This indicates that the replacement reaction is initiated locally rather than over the entire surface. As a result, after 10 min heating major products are hollow Ag-Au alloy nanoparticles under Ar gas bubbling. In continuous ageing process, the Ag-Au alloy shell becomes very thin and fall apart into discrete nanoparticles for 30–60 min heating. During the initial stage of galvanic replacement reactions, a thin layer of Au is formed on the surface of the Ag template. Assuming that the deposited layer of Au can prevent the Ag underneath from being oxidized, a pinhole can serve as the active site for Ag dissolution from the interior of the template, as shown in Figure 6(a). The Ag atoms must diffuse through the Au layer in order to be oxidized and dissolved from the template. Concurrent with the replacement reaction, alloying between Ag and Au occurs because the diffusion rates of Au and Ag are relatively high at 100°C [35] and the Ag-Au alloy is more stable than pure Au or Ag particles [34]. In the Ag-Au system, vacancies are formed because of a difference in diffusion rate for the two components. Although interdiffusion between Au and Ag occurs in our system as well, the formation of a hollow interior can be primarily attributed to the template engaged replacement reaction, where Ag leaves the template owing to oxidation as perforated and ribbon-type particles for 60 min heating.

Figure 6(b) shows schematic process for shape, size, and composition changes from Ag nanoparticles to Ag-Au alloy particles under O_2 gas bubbling after heating at 150°C for 10–60 min. As Ag seeds, spherical Ag nanoparticles with average size of 32 ± 12 nm are used. After injection of $HAuCl_4$ solution to Ag seeds solution in the presence of PVP under O_2 gas bubbling, more rapid shape changes occur. Spherical Ag seeds change to ring-type particles with a pin hole at upper surface area. Pin holes becomes large by occurrence of more replacement reaction. In this reaction stage, a small amount of ribbon-type particles is formed due to fast oxidative etching of Ag sacrificial template by O_2/Cl^- and by the replacement reaction between Ag atoms and $AuCl_4^-$. Therefore, Ag particles are oxidized and dissolved as Ag^+ ions in solution at 150°C. The dissolved Ag^+ ions

are rereduced by EG to small (<5 nm) spherical particles. After 60 min heating, the residual perforated particles are drastically split off into discrete nanoparticles or (collapsed into small fragments) ribbon-type particles.

The shape and composition of final products are different depending on the bubbling gas, Ar or O_2. In case of Ar bubbling, ring-like perforated Ag-Au alloy particles and some fragment species are produced. On the other hand, the major products are discrete (ribbon-type) Au rich Ag-Au alloy particles because of rapid shape, size, and composition changes under O_2 bubbling. These findings show that the shape, size, and composition could be controlled by changing bubbling gas in the Ag-$AuCl_4^-$ galvanic replacement reaction.

4. Conclusion

In summary, we have demonstrated that a change between Ag oxidation and Au deposition in galvanic replacement reactions by changing bubbling gas can lead to differences in the morphology, composition, and optical properties of the resultant hollow nanostructures. When spherical and decahedron Ag particles are heated with $HAuCl_4$/PVP/EG solution at 150°C under Ar and O_2 gas bubbling, different types of Ag-Au alloy particles are formed at the early stages of galvanic replacement reaction. More drastic shape, size, and composition changes in products are observed under O_2 bubbling than those under Ar bubbling. Major products are ring-like Ag-Au alloy particles with minor amount of ribbon particles under Ar gas bubbling, whereas spherical Ag templates rapidly turn to thin wall ring-like particles and small ribbon-type particles under O_2 bubbling. UV-visible spectroscopy, TEM, and TEM-EDS all confirmed the formation of homogeneous Ag-Au alloy nanoparticles. The alloy nanoparticles are formed by the rapid interdiffusion of Au and Ag atoms as a result of the reduced dimension of the Ag nanoparticles, operating temperature, and the large number of interfacial vacancy defects generated by the replacement reaction under O_2 gas bubbling. The method used in this study has several notable advantages such as the ease of independent control of both size and composition of the alloy nanoparticles and the production of the alloy nanoparticles in relatively high concentrations. This method is a versatile method for synthesizing Ag-Au alloy nanostructures as well as tuning their LSPR peaks for use in controlled release of drugs, optical sensing, and photothermal therapy.

Acknowledgments

This work was supported by JSPS KAKENHI Grant nos. 22310060 and 25286003, by the Management Expenses Grants for National Universities Corporations from the MEXT, and Kyushu University GCOE program "Novel Carbon Resource Sciences." Md. Jahangir Alam gratefully acknowledges a Kuma Scholarship and the Graduate School of Engineering Science, Kyushu University, for the financial support.

References

[1] S. Sun, C. B. Murray, D. Weller, L. Folks, and A. Moser, "MonodisperseFePt nanoparticles and ferromagnetic FePt nanocrystal superlattices," *Science*, vol. 287, no. 5460, pp. 1989–1992, 2000.

[2] N. Toshima, M. Harada, Y. Yamazaki, and K. Asakura, "Catalytic activity and structural analysis of polymer-protected gold-palladium bimetallic clusters prepared by the simultaneous reduction of hydrogen tetrachloroaurate and palladium dichloride," *Journal of Physical Chemistry*, vol. 96, no. 24, pp. 9927–9933, 1992.

[3] J.-H. Liu, A.-Q. Wang, Y.-S. Chi, H.-P. Lin, and C.-Y. Mou, "Synergistic effect in an Au–Ag alloy nanocatalyst: CO oxidation," *Journal of Physical Chemistry B*, vol. 109, no. 1, pp. 40–43, 2005.

[4] A.-Q. Wang, J.-H. Liu, S. D. Lin, T.-S. Lin, and C.-Y. Mou, "A novel efficient Au–Ag alloy catalyst system: preparation, activity, and characterization," *Journal of Catalysis*, vol. 233, no. 1, pp. 186–197, 2005.

[5] P. Mulvaney, "Surface plasmon spectroscopy of nanosized metal particles," *Langmuir*, vol. 12, no. 3, pp. 788–800, 1996.

[6] S. Link, Z. L. Wang, and M. A. El-Sayed, "Alloy formation of gold-silver nanoparticles and the dependence of the plasmon absorption on their composition," *Journal of Physical Chemistry B*, vol. 103, no. 18, pp. 3529–3533, 1999.

[7] M. P. Mallin and C. J. Murphy, "Solution-phase synthesis of sub-10 nm Au–Ag alloy nanoparticles," *Nano Letters*, vol. 2, no. 11, pp. 1235–1237, 2002.

[8] O. M. Wilson, R. W. J. Scott, J. C. Garcia-Martinez, and R. M. Crooks, "Synthesis, characterization, and structure-selective extraction of 1–3-nm diameter AuAg dendrimer-encapsulated bimetallic nanoparticles," *Journal of the American Chemical Society*, vol. 127, no. 3, pp. 1015–1024, 2005.

[9] S. Senapati, A. Ahmad, M. I. Khan, M. Sastry, and R. Kumar, "Extracellular biosynthesis of bimetallic Au–Ag alloy nanoparticles," *Small*, vol. 1, no. 5, pp. 517–520, 2005.

[10] M. J. Hostetler, C.-J. Zhong, B. K. H. Yen et al., "Stable, monolayer-protected metal alloy clusters," *Journal of the American Chemical Society*, vol. 120, no. 36, pp. 9396–9397, 1998.

[11] N. N. Kariuki, J. Luo, M. M. Maye et al., "Composition-controlled synthesis of bimetallic gold-silver nanoparticles," *Langmuir*, vol. 20, no. 25, pp. 11240–11246, 2004.

[12] D.-H. Chen and C.-J. Chen, "Formation and characterization of Au–Ag bimetallic nanoparticles in water-in-oil microemulsions," *Journal of Materials Chemistry*, vol. 12, no. 5, pp. 1557–1562, 2002.

[13] A. B. Smetana, K. J. Klabunde, C. M. Sorensen, A. A. Ponce, and B. Mwale, "Low-temperature metallic alloying of copper and silver nanoparticles with gold nanoparticles through digestive ripening," *Journal of Physical Chemistry B*, vol. 110, no. 5, pp. 2155–2158, 2006.

[14] Y.-H. Chen and C.-S. Yeh, "A new approach for the formation of alloy nanoparticles: laser synthesis of gold-silver alloy from gold-silver colloidal mixtures," *Chemical Communications*, no. 4, pp. 371–372, 2001.

[15] I. Lee, S. W. Han, and K. Kim, "Production of Au–Ag alloy nanoparticles by laser ablation of bulk alloys," *Chemical Communications*, no. 18, pp. 1782–1783, 2001.

[16] A. T. Izgaliev, A. V. Simakin, and G. A. Shafeev, "Formation of the alloy of Au and Ag nanoparticles upon laser irradiation of the mixture of their colloidal solutions," *Quantum Electronics*, vol. 34, no. 1, pp. 47–50, 2004.

[17] G. C. Papavassiliou, "Surface plasmons in small Au–Ag alloy particles," *Journal of Physics F*, vol. 6, no. 4, pp. L103–L105, 1976.

[18] Y. Sun, B. T. Mayers, and Y. Xia, "Template-engaged replacement reaction: a one-step approach to the large-scale synthesis of metal nanostructures with hollow interiors," *Nano Letters*, vol. 2, no. 5, pp. 481–485, 2002.

[19] H.-P. Liang, L.-J. Wan, C.-L. Bai, and L. Jiang, "Gold hollow nanospheres: tunable surface plasmon resonance controlled by interior-cavity sizes," *Journal of Physical Chemistry B*, vol. 109, no. 16, pp. 7795–7800, 2005.

[20] P. R. Selvakannan and M. Sastry, "Hollow gold and platinum nanoparticles by a transmetallation reaction in an organic solution," *Chemical Communications*, no. 13, pp. 1684–1686, 2005.

[21] Y. Sun and Y. Xia, "Mechanistic study on the replacement reaction between silver nanostructures and chloroauric acid in aqueous medium," *Journal of the American Chemical Society*, vol. 126, no. 12, pp. 3892–3901, 2004.

[22] Y. Sun and Y. Xia, "Increased sensitivity of surface plasmon resonance of gold nanoshells compared to that of gold solid colloids in response to environmental changes," *Analytical Chemistry*, vol. 74, no. 20, pp. 5297–5305, 2002.

[23] Y. Sun, B. Mayers, and Y. Xia, "Metal nanostructures with hollow interiors," *Advanced Materials*, vol. 15, no. 7-8, pp. 641–646, 2003.

[24] Y. Sun and Y. Xia, "Multiple-walled nanotubes made of metals," *Advanced Materials*, vol. 16, no. 3, pp. 264–268, 2004.

[25] G. S. Métraux, Y. C. Cao, R. Jin, and C. A. Mirkin, "Triangular nanoframes made of gold and silver," *Nano Letters*, vol. 3, no. 4, pp. 519–522, 2003.

[26] W. Lin, T. H. Warren, R. G. Nuzzo, and G. S. Girolami, "Surface-selective deposition of palladium and silver films from metal-organic precursors: a novel metal-organic chemical vapor deposition redox transmetalation process," *Journal of the American Chemical Society*, vol. 115, no. 24, pp. 11644–11645, 1993.

[27] L. A. Porter Jr., H. C. Choi, A. E. Ribbe, and J. M. Buriak, "Controlled electroless deposition of noble metal nanoparticle films on germanium surfaces," *Nano Letters*, vol. 2, no. 10, pp. 1067–1071, 2002.

[28] X. Lu, H.-Y. Tuan, J. Chen, Z.-Y. Li, B. A. Korgel, and Y. Xia, "Mechanistic studies on the galvanic replacement reaction between multiply twinned particles of Ag and $HAuCl_4$ in an organic medium," *Journal of the American Chemical Society*, vol. 129, no. 6, pp. 1733–1742, 2007.

[29] X. Tang, M. Tsuji, M. Nishio, and P. Jiang, "Roles of chloride anions in the shape evolution of anisotropic silver nanostructures inpoly(vinylpyrrolidone) (PVP)- assisted polyol process," *Bulletin of the Chemical Society of Japan*, vol. 82, no. 10, pp. 1304–1312, 2009.

[30] B. Wiley, T. Herricks, Y. Sun, and Y. Xia, "Polyol synthesis of silver nanoparticles: use of chloride and oxygen to promote the formation of single-crystal, truncated cubes and tetrahedrons," *Nano Letters*, vol. 4, no. 9, pp. 1733–1739, 2004.

[31] M. Hu, J. Chen, Z.-Y. Li et al., "Gold nanostructures: engineering their plasmonic properties for biomedical applications," *Chemical Society Reviews*, vol. 35, no. 11, pp. 1084–1094, 2006.

[32] B. J. Wiley, S. H. Im, Z.-Y. Li, J. McLellan, A. Siekkinen, and Y. Xia, "Maneuvering the surface plasmon resonance of silver nanostructures through shape-controlled synthesis," *Journal of Physical Chemistry B*, vol. 110, no. 32, pp. 15666–15675, 2006.

[33] L. Lu, H. Wang, Y. Zhou et al., "Seed-mediated growth of large, monodisperse core-shell gold-silver nanoparticles with Ag-like optical properties," *Chemical Communications*, no. 2, pp. 144–145, 2002.

[34] H. Shi, L. Zhang, and W. Cai, "Composition modulation of optical absorption in Ag_xAu_{1-x} alloy nanocrystals in situ formed within pores of mesoporous silica," *Journal of Applied Physics*, vol. 87, no. 3, pp. 1572–1574, 2000.

[35] G. Ouyang, X. Tan, C. X. Wang, and G. W. Yang, "Physical and chemical origin of size-dependent spontaneous interfacial alloying of core-shell nanostructures," *Chemical Physics Letters*, vol. 420, no. 1–3, pp. 65–70, 2006.

[36] K. Dick, T. Dhanasekaran, Z. Zhang, and D. Meisel, "Size-dependent melting of silica-encapsulated gold nanoparticles," *Journal of the American Chemical Society*, vol. 124, no. 10, pp. 2312–2317, 2002.

[37] H. Yasuda and H. Mori, "Spontaneous alloying of zinc atoms into gold clusters and formation of compound clusters," *Physical Review Letters*, vol. 69, no. 26, pp. 3747–3750, 1992.

[38] H. Yasuda, H. Mori, M. Komatsu, and K. Takeda, "Spontaneous alloying of copper atoms into gold clusters at reduced temperatures," *Journal of Applied Physics*, vol. 73, no. 3, pp. 1100–1103, 1993.

[39] M. Tsuji, C. Shiraishi, M. Hattori et al., "Rapid spontaneous alloying between Pd nanocubes and Ag nanoparticles in aqueous solution at ambient temperature," *Chemical Communications*, 2013.

[40] S. K. Wonnell, J. M. Delaye, M. Bibolé, and Y. Limoge, "Activation volume for the interdiffusion of Ag-Au multilayers," *Journal of Applied Physics*, vol. 72, no. 11, pp. 5195–5205, 1992.

[41] Y. Ding and J. Erlebacher, "Nanoporous metals with controlled multimodal pore size distribution," *Journal of the American Chemical Society*, vol. 125, no. 26, pp. 7772–7773, 2003.

[42] T. Shibata, B. A. Bunker, Z. Zhang, D. Meisel, C. F. I. Vardeman, and J. D. Gezelter, "Size-dependent spontaneous alloying of Au–Ag nanoparticles," *Journal of the American Chemical Society*, vol. 124, no. 40, pp. 11989–11996, 2002.